Research Article

Considering the use of niobium and titanium to enhance electrical and mechanical properties of copper at higher operational temperature application

Azunna Agwo Eze[1] · Tamba Jamiru[1] · Emmanuel Rotimi Sadiku[2] · Mondiu Olayinka Durowoju[3] · Williams Kehinde Kupolati[4] · Idowu David Ibrahim[1]

Abstract

Electrical energy transmission materials (cables) are required to have a good combination of high-strength and high electrical conductivity properties, to avoid loss of electrical power between places of production and places of usage. In this study, pure Copper (Cu), Niobium (Nb) and Titanium (Ti) powders of the same purity and particles sizes of 99.0% and − 325 meshes respectively, were used. Niobium and titanium were added to the matrix of pure copper to form the specimens (Cu-2wt% Nb, Cu-5wt% Nb, Cu-2 wt% Ti and Cu-5wt% Ti), were consolidated at sintering temperature of 650 °C by the use of spark plasma sintering (SPS) techniques. Their electrical conductivity, densities, relative densities, hardness, corrosion, wear resistance and microstructure was investigated in this study. The results show that addition of 2 and 5 volume percent of Nb improved the electrical conductivity of Cu at elevated temperature, strength, corrosion and wear resistance of Cu better than that of titanium. Also addition of 2 volume percent of Ti was observed to improve the electrical conductivity of Cu and was stable at elevated temperature just like Cu-2wt% Nb and Cu-5wt% Nb. However, the study revealed that niobium addition to Cu will give better electrical conductivity and mechanical properties improvement than titanium in electrical cables applications.

Keywords Electrical energy transmission materials · High electrical conductivity · Hardness Vickers · Shrinkage rate

1 Introduction

Rising population of human beings and advancing technology create hug needs for electrical energy. Electricity is not for all time used within the same area where it is created, a long distance transmission cables and distribution structures are needed to transport the electrical energy to the area where it can be used. Copper and aluminum cables and wires are commonly used to transmit electrical power across long distances as high tension power lines and medium voltage lines [1]. Pure copper alone as electrical cables carrying high current, surfers a massive draw back due to its low temperature operating condition. Copper conducts electricity, but losses it electrical conductivity at higher temperature operation. Copper wire or cables drop electrical energy owing to Joule effect, which is an expanded heat resulted from current passing through a copper cables and wires [1]. When electrical current flowing through a copper increases its temperature, the excess heat passes away as wasted energy. This however, moved up design planning for overhead and underground cables for long distance transmission,

✉ Azunna Agwo Eze, ezeaaben@gmail.com; ezeaa@tut.ac.za| [1]Department of Mechanical Engineering, Mechatronics and Industrial Design, Tshwane University of Technology, Pretoria, South Africa. [2]Institute of Nano Engineering Research (INER) and Department of Chemical, Metallurgical and Materials Engineering, Tshwane University of Technology, Pretoria, South Africa. [3]Department of Mechanical Engineering, LadokeAkintola University of Technology, Oyo, Nigeria. [4]Department of Civil Engineering, Tshwane University of Technology, Pretoria, South Africa.

SN Applied Sciences (2019) 1:74 | https://doi.org/10.1007/s42452-018-0080-1

Received: 16 July 2018 / Accepted: 22 November 2018 / Published online: 29 November 2018

which will deliver energy from the step-down substation to the consumer without much loss of electrical energy [1]. However, the common way of increasing high operational temperature and strength of copper while retaining its high electrical conductivity is alloying with a possible element within the family of Body Centered Cubic (bcc) structural elements like; Cr, W, Ta, Nb, Mo, V [2–4]. Among the copper-based alloy of bcc families, Cu–Nb alloys have been reported to have the best mechanical properties [4], and It was also reported that the electrical and mechanical properties of Cu–Nb significantly surpass those of competitive alloys such as Cu–Ti, Cu–Be, and Cu–Ni-Mg [5]. Electricity itself is an electromagnetic phenomenon in nature, its generation, transmission, and utilization; all depended on the physics of electromagnetism [6], which occurred in electrical conductors. Electrical conductors with improved mechanical and electrical properties are then essential to create high pulsed magnetic fields with long pulse duration [7]. Cu–Nb high strength cable and wires are currently attractive candidates for the windings of high field pulsed magnets because they combine good electrical conductivity and high strength [8–11]. The combination of high electrical conductivity with high mechanical strength at elevated temperature is often required simultaneously for conducting materials used in transmission and distribution of electrical energy to avoid energy loses [12]. However, researches on Cu–Nb and Cu–Ti alloys have gain prevalent attention because of their properties such as high strength; excellent electrical conductivity, superior corrosion resistivity at elevated temperature. Also Cu–Nb has superior wear resistance than Cu–Ti. There are many sizeable amounts of research work in the investigation of the microstructure, mechanical properties and electrical properties of Cu–Ti alloys [13–25], and Cu–Nb alloys [5,12,26–31], with the major aim of developing a replacement for the expensive and deadly Cu-Be alloys for strength and conductivity. The aim of this work is to improve the electrical conductivity of copper at elevated temperature applications in other words; to avoid the common Joule effects which copper cables suffers when used to transmit electrical energy. In this study, spark plasma sintering (SPS) was used to consolidate the Cu, Cu-2wt% Ti, Cu-2wt% Nb, Cu-5wt% Ti and Cu-5wt% Nb alloys. The following investigation was carried out; electrical conductivity against increase of temperature, determinations of shrinkage (displacement) rate versus time of the powders during sintering at 650 °C, densities, relative densities, hardness Vickers, Scanning electron microscopy (SEM), energy dispersive x-ray spectrometer (EDS), X-ray diffraction (XRD), corrosion and wear resistivity of the sintered samples. The aforementioned tested properties of the tested samples were compared to each other in order to ascertain between Nb and Ti which one offered better improvement to Cu in terms of combined electrical conductivity and mechanical properties at elevated temperature, for efficient transmission and distribution applications.

2 Experimental procedure

2.1 Materials and methods

The starting powders used in this study are Copper (Cu), Niobium (Nb) and Titanium (Ti) of the same purity and particles sizes of 99.0% and − 325 meshes (~ − 44 microns), supplied by Alfa Aesar. Samples of Cu-based alloys containing 2 and 5 wt% Nb and Ti in the composition of Cu-2wt% Nb, Cu-5wt% Nb, Cu-2wt% Ti, Cu-5wt% Ti and pure Cu (reference material) were prepared and mixed in the region of Cu-solid solution. The four prepared Cu-based powdered alloys were separately inserted in a plastic cylinder with balls of alumina and mixed for two hours in turbular shaker mixer apparatus for 72 rpm.

The electrical resistivity test against increase in temperature, were determined by the use of the spark plasma sintering (SPS) machine HHPD25 from FCT Germany. The reported electrical conductivity values (Eq. 1), were the reciprocal of the recorded resistivity values of the tested samples. The use of SPS machine in determining the electrical resistivity behavior of the samples, have the advantage of overcoming electrode effect, which is a common problem in the conventional electrical conductivity testing instruments. However, during the electrical resistivity test of the samples, clean Cu (reference material) and the blended powdered alloys of 2 and 5 wt% titanium and Nb were put inside non-conductive Silicon nitrate (Si_2N_4) die of 2cm diameter and height of 0.2 cm, and were connected with Molybdenum punch that has a copper base (serves as the electrode). Electrical contact between the powder particles was achieved through functional compacted load of 10 KN. Electrical powers of 8 kilowatts was used, but as the temperature turned out to be steady, extra 2 kilowatt of electrical power were added in the time interval of 2 min. The test was stopped just before the commencement of sintering, so that the measured resistivity will be that of the powder and not the sintered materials.

$$\delta = \frac{1}{\rho} \tag{1}$$

where δ represent electrical conductivity and ρ represent the electrical resistivity.

The spark plasma sintering (SPS) machine HHPD25 from FCT Germany was used for the electrical conductivity test and full sintering of all the samples at

temperature of 650 °C, heating rate of 50 °K per minutes, dwelling time of 5 min and pressure of 60 MPa. All the sintered samples were grinded and polished, their morphology were studied using Field Emission Scanning Electron Microscopy (SEM) (JEOL, JSM-7600f) which was incorporated with energy dispersive x-ray spectrometer (EDS) detectors. A model PANalytical EMPYREA X-ray diffraction (XRD) readings were carried out, using a CuKα radiation for phase analysis, with X'PertHighScore Plus software. Images were captured at an accelerating voltage of 15 kV and a probe current of 0.5×10^{-9} A. The experimental densities were reported as the arithmetic mean of four different measurements taken from the same sample, and the relative densities of the sintered samples were also determined. The micro-hardness was measured using a Vickers indentation method at applied load of 100 Gramm force with holding time of 10 s, and the test result for each sample was the arithmetic mean of 5 successive indentations with standard deviations.

Electrochemical studies were therefore carried out in 1 mol of Sulphuric acid (H_2SO_4) solution environment that contained the solid sintered samples (working electrode), counter electrode which is made up of graphite and saturated Silver/ Silver chloride which served as reference electrode. The corrosion tests were carried out with VersaSTAT four with versa studio four software. Potentiodynamic polarization procedure was used to review the general electrochemical behavior of the sintered samples of Cu, Cu-2wt% Ti, Cu-2wt% Nb, Cu-5wt% Nb and Cu-5wt% Ti alloys. Prior to the scanning, every one of the tested samples were immersed in the electrolyte for 4 min to permit them to become stable before the open circuit potential measurement, which was done for about two hours. Every one of the samples tested was scanned at a scan rate of 2 mV/s with potential variety from 0.5 to 1.5 V.

Tribological behavior of the sintered samples in a reciprocating dry sliding condition was conducted using a CETR-2-UMT tribometer provided with a computer controlled ball-on-disk arrangement that operated under room temperature. A 1cm diameter counter surface ball of tungsten carbide (WC) was employed to slip against the tested samples in a countered motion, in a load of 25 N and at a frequency of 5 Hz. A perpendicularly downwards load was used on the samples tested, with a motor-driven moving parts that operated a load measuring device for the reaction in order to maintain a steady applied load. The coefficient of friction (μ) was constantly recorded during the sliding operation and the results were obtained from the UMT-2-CETR apparatus software.

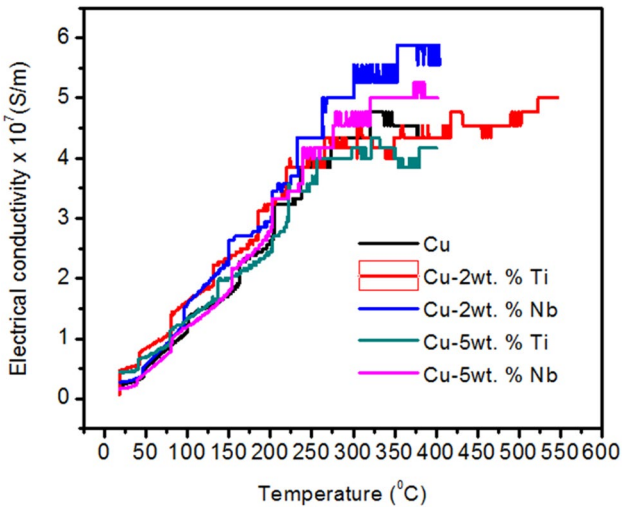

Fig. 1 Variations in electrical conductivity with increased temperature of clean Cu, Cu-2wt% Ti, Cu-2wt% Nb, Cu-5wt% Ti and Cu-5wt% Nb alloys

Table 1 Summary of the results of the electrical conductivity with temperature of the samples

Tested samples	Electrical conductivity (S/m)	Temperature (°C)
Cu-2wt% Nb	5.91×10^7	403
Cu-5wt% Nb	5.30×10^7	386
Cu-2wt% Ti	5.10×10^7	545
Cu	4.77×10^7	334
Cu-5wt% Ti	4.36×10^7	328

3 Results and discussion

3.1 Electrical conductivity with increased temperature of the samples

In this study of electrical conductivity with increasing temperature measurements of the studied samples (Fig. 1), every sample tested was clogged at an end where the electrical conductivity stopped to raises with temperature. Figure 1 demonstrated the disparity in electrical conductivity among Cu-5wt% Nb, Cu-5wt% Ti, Cu-2wt% Nb, Cu-2wt% Ti alloys and clean Cu powders with increased in temperature. Table 1 shows the results of the electrical conductivity versus the temperatures, which is arranged based on the best electrical conductivity with temperature of the samples.

The clarification of the incident that effected in a diminution in electrical conductivity of clean Cu beyond 334 °C, may perhaps be the evident of phonons

introduction, which is the perfect resistivity of the materials. Within clean metals like in pure Cu, phonons are responsible for the scattering of electrons by means of the exciting lattice ion of the metal, owing to elevated thermal energy engaged within the atom. When electrical current flows in the conductor, the temperature of the metal increase, thermal energy will be stimulated and this will cause the ions in the atoms to move out of their stable location, thus, hindering the free moving electrons in the conductors. Effect of phonon is insignificant at ~20 °C because the ions are kept in their secured position in the lattice of the atoms. On the other hand, metals can conduct electricity provided their ions continued to remain stable in their lattice, devoid of being disorderly of the free movement of the electrons, which are charged carriers [32]. The electrical conductivity of Cu-2wt% Nb and Cu-5wt% Nb alloys was observed to be higher than that of clean Cu, Cu-2wt% Ti, and Cu-5wt% Ti alloys counterparts. Their electrical conductivity was seen to be more stable at higher temperatures than others (Cu, Cu-2wt% Ti and Cu-5wt% Ti alloys); the high temperature stability observed in Cu-2wt% Nb and Cu-5wt% Nb alloys was attributed to the presence of Nb in the Cu matrix. This phenomenon is in line with thermal conductivity behavior of Nb, that its particles show high temperature stability [33]. The high electrical conductivity observed in Cu-2wt% Nb could be attributed to; high electrical conductivity of Nb, lower weight percent content of Nb which dissolved in Cu matrix, as temperatures increases the dissolved particles of Nb served as heat absorber that absorbed the excess heat energy and decreases the scattering to electrons and benefit the enhancement of the electrical conductivity of Cu [34]. On the other hand, high electrical conductivity with increased in temperature was also observed in Cu-2wt% Ti which was higher than that of clean Cu and Cu-5wt% Ti alloy. These phenomena are considered to result from decreases in the amount of the dissolved titanium (Ti) by precipitation [25] in Cu-2wt% Ti alloy. However, the high electrical conductivities with temperature sustained by Cu-2wt% Nb and Cu-2wt% Ti which was above their 5% (Cu-5wt% Nb and Cu-5wt% Ti), could be that at high temperature, the low 2% of Nb and Ti would dissolved in the solution with Cu, thereby enhanced electrical conductivity and strength.

However, to summarize the Electrical conductivity against the increase of temperature of the samples is shown in Fig. 1. Figure 1 shows the variation of electrical conductivity with temperature for all the samples considered in this work. It can be observed from the graph that at the temperature increases (25–550 °C), the electrical conductivity also increases. This can be attributed to the increased number of free electrons required for electrical conductivity. In the temperature range 25–550 °C, there is a slight improvement in the electrical conductivity of Cu-2wt% Nb and Cu-2wt% Ti alloys over that of other samples. This shows that in this temperature range, the lower the amount of Nb and Ti the better the electrical conductivity [25]. Above 300 °C, interesting results showing the effects of the type of alloying elements (Nb or Ti) and the amount added to the alloy (2 or 5%) were obtained. It was noticed that Cu-2wt% Nb alloy had the highest value of electrical conductivity followed by Cu-5wt% Nb alloy. This observation shows that if improvement in electrical conductivity of copper is desired, it is better to add Nb instead of Ti.

3.2 Shrinkage rate of the sintered powders versus time

The shrinkage rate curves (Fig. 2) was used for the explanation of densification mechanisms of the powders during sintering at a temperature of 650 °C, under the punch compressive load of 60 MPa, holding time of 5 min and heating rate of 50 °K/min. The shrinkage/displacement rate of the powdered particles during spark plasma sintering, determined the densification nature of the sintered sample and it has direct relationship with the microstructure, density, relative density and micro hardness of the sintered sample. In Fig. 2, it can be seen that the speed at which the pure copper particles shrink per time inside a graphite die, was higher compared to the rest of sintered samples. Pure copper has one sharp peak which occurred at 25 min, it can also be observed that each Cu-2wt% Nb and Cu-5wt% Nb has one sharp peak. Figure 2 also shows that the shrinkage rate of Cu-2wt% Nb and Cu-5wt% Nb powders was higher than that of

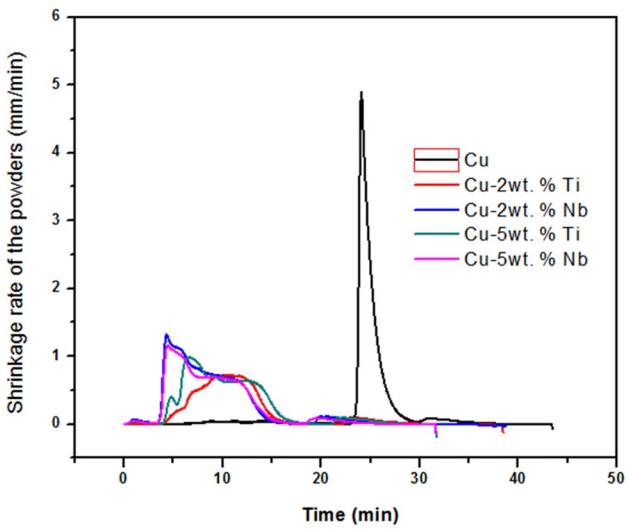

Fig. 2 The shrinkage rate versus time for Cu, Cu-2wt% Ti, Cu-2wt% Nb, Cu-5wt% Ti and Cu-5wt% Nb sintered at 650 °C

Cu-5wt% Ti and Cu-2wt% Ti powders. Sharp peak and high shrinkage rate of powdered particles observed in Cu, Cu-2wt% Nb and Cu-5wt% Nb can be attributed to their electrical type (conductive materials). However, in conductive powder, heating of the particles are mainly due to the Joule effect and for the non-conductive powder like Ti, heating occurs through heat transfer from the die and compressive punches [35]. The Joule effect will initiate rapid heating which can effectively suppress particle coursing and thus favors intensive particle rearrangement [36]. However, densification by particle rearrangement takes place rather rapidly because grains rather than atoms act as the migrating units [36], shrinkage rate of the powdered particle is governed by capillary forces developed in the grain boundary [37], and this information may clarify the observed confirmation of significant higher shrinkage rate and sharp peak found in Cu, Cu-2wt% Nb and Cu-5wt% Nb. This outcome showed that the presence of Cu and Nb as conductive path allows a faster particle rearrangement during the spark plasma sintering at 650 °C.

3.3 Microstructure, density, relative density, micro hardness and x-ray pattern of the fully sintered samples at 650°C

After full sintering of the tested samples at sintered temperature of 650 °C, dwelling time of 5 min, compressive punch load of 60 MPa, and heating rate of 50 °K/min. The change in microstructure, density, relative density, micro hardness and x-ray pattern as a function of the abovementioned spark plasma sintered (SPS) parameters, are shown in (Figs. 3, 4, 5 and Table2) which summaries the aforementioned properties. Figure 3 shows the scanned electron microscopy (SEM) images, with their energy dispersive x-ray spectrometer (EDS) graph; (a) Clean Cu (b) Cu-2wt% Nb (c) Cu-5wt% Nb (d) Cu-2wt% Ti and (e) Cu-5wt% Ti. In Fig. 3a, it can be seen that there was an even distribution of Cu particles all over the sintered sample, and it is an indication of full densification during sintering (Fig. 2). The EDS graph showed only Cu, which confirmed that there were no contaminations during the sintering process. This explains why it recorded the highest density and relative density observed in Fig. 4a, b, and Table 2. In Fig. 3b, there

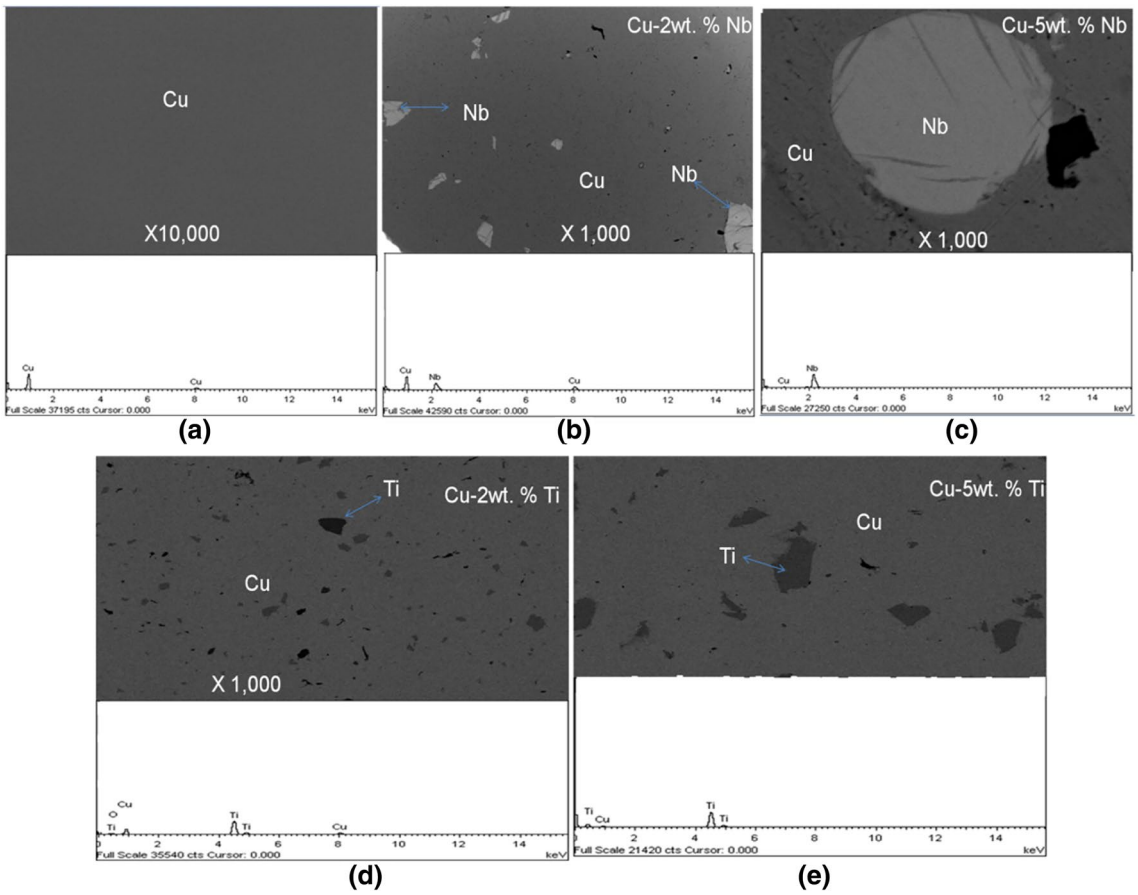

Fig. 3 SEM images with ED's graph of fully sintered at temperature of 650 °C; **a** Clean Cu **b** Cu-2wt% Nb **c** Cu-5wt% Nb **d** Cu-2wt% Ti and **e** Cu-5wt% Ti alloys

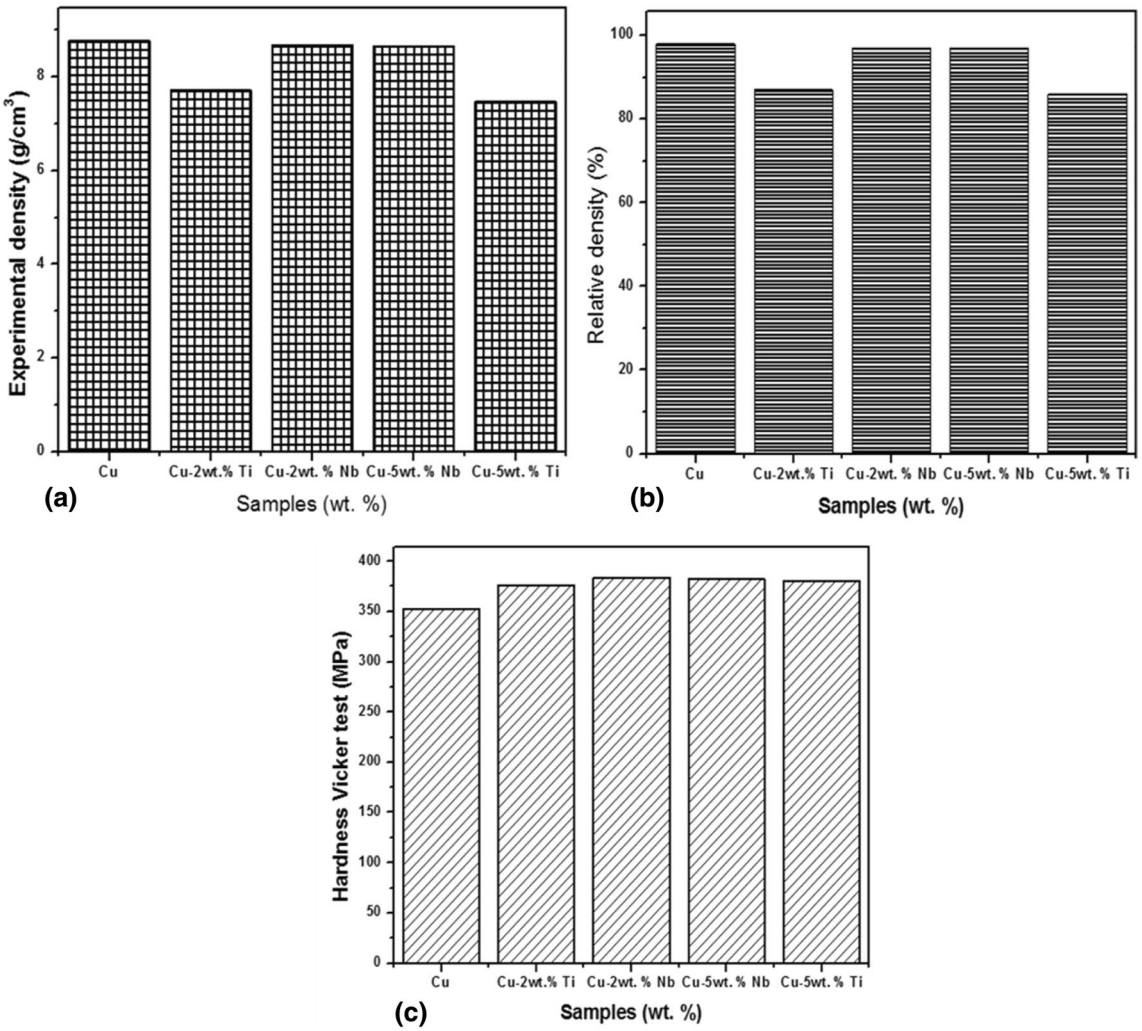

Fig. 4 Graphs of Cu, Cu-2wt% Ti, Cu-2wt% Nb, Cu-5wt% Nb and Cu-5wt% Ti; **a** experimental density **b** relative density and **c** Vickers hardness of the fully sintered samples at temperature of 650 °C

are precipitate of Nb particles observed, which is gray in color and was dispersed over the body of the alloy (Cu-2wt% Nb). The EDS graph of the entire alloy showed the presence of Cu and Nb only, confirming the maintenance of its purity from powders mixing to sintering process. These could be the reason of high density, relative density, hardness and electrical conductivity it recorded over the rest of the alloys. In Fig. 3c, precipitate of big Nb particles was observed and it was situated at the center of Cu-5wt% Nb alloy. The big precipitate of Nb particles formed, may be attributed to poor dissolution of large amount of Nb particles in solid solution of Cu, and prevented evenly dispersion of the Nb particles during the turbular mixing of the powders. The clustered Nb particles could have been the reason for the slight reduction in properties of Cu-5wt% Nb alloy compared to that of Cu-2wt% Nb alloy. The alloy (Cu-5wt% Nb) maintained its purity throughout the process as seen in the EDS graph of the entire alloy (Fig. 3c). In Fig. 3d, it can be seen that small particles of Ti was seen dispersed in the matrix of Cu after sintering. The EDS of a big black pigment in Fig. 3d shows the presence of Ti and oxygen, the presence of oxygen is as a result of the oxidation of Ti and also indicated the presence of pores at that part of the alloy. The presence of pores could be the reason for low densification during sintering at sintering temperature of 650 °C. In the SEM of Cu-5wt% Ti alloy (Fig. 3e), precipitate of an irregular shaped particles of Ti was observed, which was randomly dispersed in the matrix of Cu. The EDS graph of the big irregular shaped black pigment shows the presence of Ti alone, these proved that there were no contaminations encountered by the alloy during powder mixing and sintering process. Figure 4 shows the; (a) experimental density (b) relative density, and (c) hardness Vickers of the fully sintered samples at

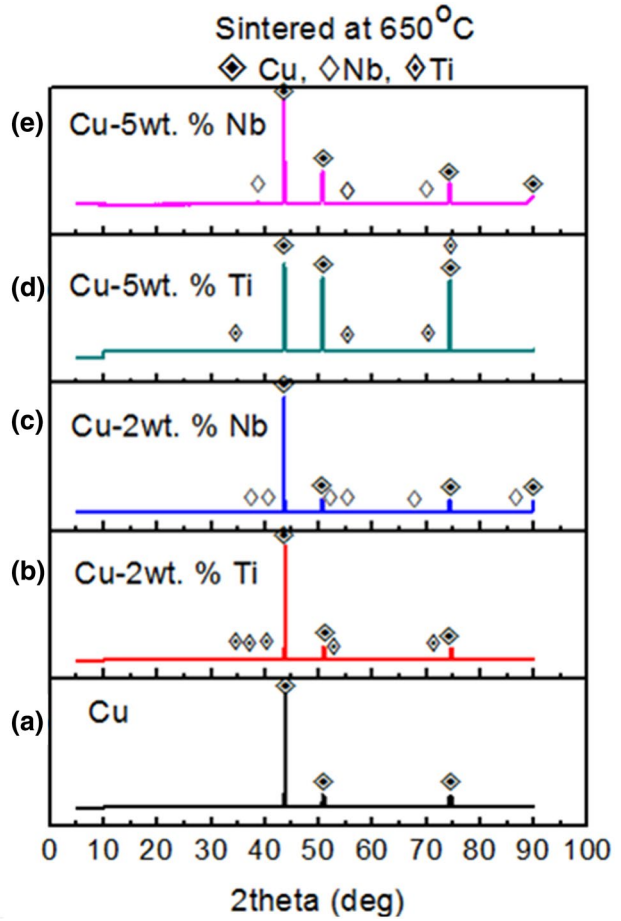

Fig. 5 XRD patterns of the fully sintered; **a** clean Cu **b** Cu-2wt% Ti **c** Cu-2wt% Nb **d** Cu-5wt% Ti, and **e** Cu-5wt% Nb alloys

650 °C. Figure 5 shows the XRD patterns for clean Cu, Cu-2wt% Ti, Cu-2wt% Nb, Cu-5wt% Ti and Cu-5wt% Nb alloys. It can be observed that the addition of 2% Nb and Ti does not make significant effects on the peak intensity of copper showing that the desired aim of improvement in properties by forming alloys with the two elements is somehow fulfilled. This has been confirmed by the improvement in mechanical and electrical properties of the alloys. The preference for Nb in terms of property improvement can also be attributed to the additional peak observed in Fig. 5c, e at 90°, 2 thetas. At 5% addition Nb and Ti, a pronounced effect of these percentage additions on the intensities and phases formed can be observed particularly with 5% Ti addition.

The XRD patterns have therefore confirmed the observed changes in properties noticed in this study [34,38].

Table 2 shows the summary of the density, relative density and micro hardness of the sintered samples at 650 °C.

3.4 Corrosion behavior of the sintered samples

Figure 6 showed; (a) potentiodynamic polarization and (b) Open circuit potential measurement of the studied samples, and Table 3 shows the summary of corrosion properties of the studied samples. Potentiodynamic polarization test were carried out by sweeping the potentials at a scan rate of 2 mV/s. Figure 6a shows the potentiodynamic polarization curves of sintered clean Cu, Cu-2wt% Ti, Cu-2wt% Nb, Cu-5wt% Ti and Cu-5wt% Nb alloys in 1 mol of H_2SO_4 acid solution. A characteristic polarization curve presented in Fig. 6a, disclosed a slight difference on corrosion potentials of clean Cu, Cu-2wt% Ti, Cu-2wt% Nb, Cu-5wt% Ti and Cu-5wt% Nb alloys. At the initial stage of the process, Cu-5wt% Nb alloy had the highest dissolution potential, followed by Cu-5wt% Ti alloy while the dissolution potentials of Cu-2wt% Nb was slightly less than the Cu-2wt% Ti alloy as time progressed.

The open circuit potential (OCP), is a factor which specify the thermodynamically affinity of a material to electrochemical corrosion in a corrosive medium. The OCP is used as a criterion for the corrosion behavior. Figure 6b shows the OCP curves for all the sintered samples immersed in 1 mol H_2SO_4 acid solution at room temperature. Conversely, at some stage in the first moments of immersion of the studied samples in the acid solution, Cu-5wt% Nb had the highest corrosion resistance potentials but its propensity changes showing a decline as time goes, reaching negative values. It did not exhibit potential drops associated with surface activation during more

Table 2 Summary showing the density, relative density and micro hardness of samples sintered at 650 °C

Samples composition	Composition in weight percent (wt%)			Theoretical density (g/cm^3)	Experimental density (g/cm^3)	Relative density (%)	Hardness Vickers (MPa)
	Cu	Nb	Ti				
Clean Cu	100	–	–	8.960	8.780	98.000	353.000
Cu-2Nb	98	2	–	8.952	8.680	97.000	383.760
Cu-5Nb	95	5	–	8.940	8.670	97.00	381.920
Cu-2Ti	98	–	2	8.872	7.720	87.000	376.380
Cu-5Ti	95	–	5	8.702	7.480	86.000	380.070

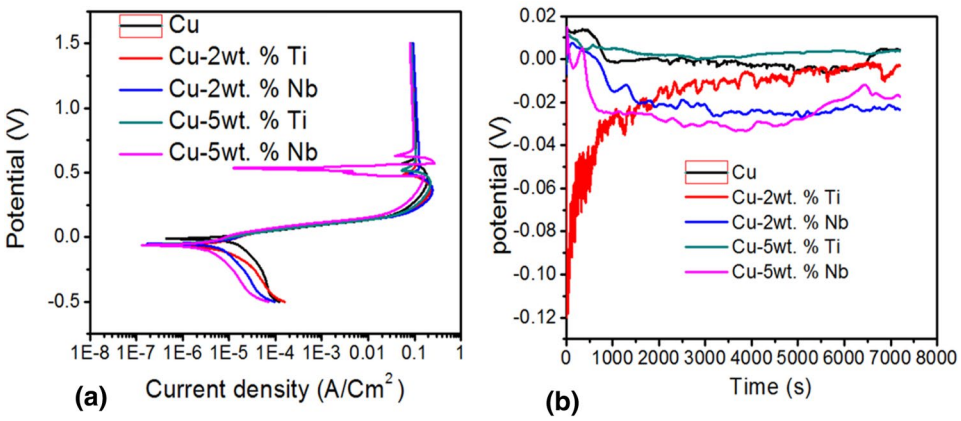

Fig.6 **a** Potentiodynamic polarization and **b** Open circuit potential measurement of the studied samples (Cu, Cu-2wt% Ti, Cu-2wt% Nb, Cu-5wt% Ti, and Cu-5wt% Nb)

Table 3 Summary of corrosion data; corrosion potential (E_{corr}), corrosion current (I_{corr}), and corrosion rate obtained from the polarization experiments

Composition in wt%	Corrosion potentials (V)	Corrosion current (A/cm^3)	Corrosion rate (mm/y)
Clean Cu	−0.012	1.635E−6	1.895E−2
Cu-2Nb	−0.051	1.830E−6	2.111E−2
Cu-5Nb	−0.063	1.040E−6	1.187E−2
Cu-2Ti	−0.059	1.609E−6	1.826E−2
Cu-5Ti	−0.062	9.157E−7	1.005E−2

than 5000 s exposure in acid solution and move in proximity to Cu-2wt% Nb and Cu-2wt% Ti alloys. These kinds of behavior of Cu-5wt% Nb strongly recommend that the air form negative oxides are thermodynamically resistant to chemical dissolution [39] in H_2SO_4 acid solution. It was also observed in Fig. 6b, that Cu-5wt% Ti alloy and clean Cu were relatively stabilized when compared with other samples. The stability in the potentials of Cu-5wt% Ti and clean Cu indicated that they were thermodynamically stable with time in 1 mol H_2SO_4 acid solution environment. Also, Cu-2wt% Ti alloy was the only sample that showed a rapid OCP displacement towards positive potentials, and became stable with increase in exposure time in the neighborhoods of clean Cu. This steady increase of potentials towards positive potentials appears to be associated with the increase formation and thickening of the oxide film on the surface of Cu-2wt% Ti alloy, developing its corrosion protection capacity. The stable corrosion resistance observed in Cu-5wt% Ti, suggested that there was good interfacial bonding between Cu and Ti particles in the alloy. There might be formation of cracks in the interfacial bonds between Cu and Nb particles in Cu-5wt% Ti and Cu-2wt% Nb alloys as time progresses, and the porosity observed in Cu-2wt% Ti (Fig. 3b–d), these cracks and pores might serve as a corrosion site which resulted to the unstable corrosion resistance observed in Fig. 6b. Table 3 shows

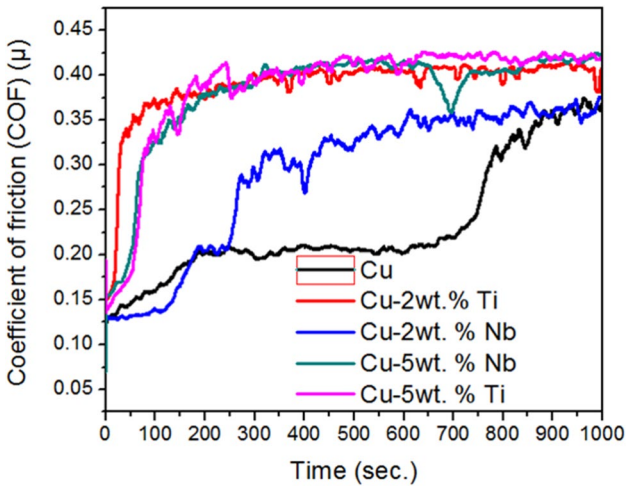

Fig. 7 Graph of Coefficient of Friction against sliding time of clean Cu, Cu-2wt% Ti, Cu-2wt% Nb, Cu-5wt% Nb and Cu-5wt% Ti alloys under the load of 25 N

the summary of corrosion data; corrosion potential (E_{corr}), corrosion current (i_{corr}), and corrosion rate obtained from the polarization experiments. In the Table 3, some conclusion can be obtained; clean Cu behaves worse compared with the rest of the alloys. Therefore, alloying with 2 and 5 volume percent of Nb and Ti improves corrosion resistance of Cu.

3.5 Wear study of the sintered samples

At the initial stage under 25 N load (Fig. 7), the variation of steady state friction coefficient for Cu-2wt% Nb alloy is the lowest at 0.13, and was maintained to 95 s before a gradual increased towards the neighborhoods of clean Cu. The coefficient of Clean Cu was observed to be 0.19 which was the lowest at 300 s, and kept steady up to 674 s before it increases towards the neighborhoods of Cu-2wt% Nb alloy. The two areas where Cu-2wt% Nb

and clean Cu intercept could be where there are only Cu particle, there are no Nb particle at that zone. Generally, the increase of coefficient of friction above that of clean Cu observed in Cu-2wt% Nb and Cu-5wt% Nb, could be attributed to weak interfacial bond that might resulted due to low sintered temperature of 650 °C, and the nature of their microstructures (the position of Nb particles in Cu matrix). Nb has been known as a material of high wear resistance. On the other hand, the high coefficient of friction observed in Cu-2wt% Ti and Cu-5wt% Ti alloys was as a result of the presence of Ti. The more volume percent Ti addition into Cu matrix, the higher the coefficient of friction the alloy will record as in Fig. 7. Therefore, addition of 2 volume percent of Nb possessed better wear resistant to Cu than addition of Ti. Addition of Ti lowered the wear resistant of Cu as it can be seen in Fig. 7.

4 Conclusion

In this study, it has been shown that the alloy of 2 and 5 wt% of Nb and Ti addition (Cu-2wt% Nb, Cu-5wt% Nb and Cu-2wt% Ti) increases the electrical conductivities of Cu at elevated temperatures. The 2 and 5 wt% of Nb and Ti addition (Cu-2wt% Nb, Cu-5wt% Nb, Cu-2wt% Ti and Cu-5wt% Ti) improved the hardness Vickers and corrosion resistivity of Cu in aH_2SO_4 acid solution environment. The presence of 2 and 5 wt% of Nb and Ti decreased the shrinkage rate of copper powdered particles during spark plasma sintering at 650 °C also altered the microstructures of Cu. It was also observed that the addition of 2 wt% Nb decreased the coefficient of friction of Cu under dry sliding conditions. In the overall results, addition of 2 wt% of Nb gave the best improvement to Cu in terms of electrical and mechanical property. With these findings, it is envisaged that Cu-2wt% Nb is the best alloy among the other alloys under investigations, and can be used in the area where Cu is required to maintain good electrical and mechanical properties at elevated temperatures, and also find applications in an acid environment, without any significant acidic attack on the materials. This study also shown that the statement of Raabe et al. [5] (that Cu–Nb alloys have mechanical and electrical conductivity properties that surpassed other Cu-based alloys including Cu–Ti alloys) was correct.

Acknowledgements The author, Eze AA and Ibrahim ID gratefully acknowledged the Council of Scientific and Industrial Research (CSIR) and the Department of Science and Technology (DST), South Africa (Grant Number: CSIR-IBS), for providing the financial support for this research.

Compliance with ethical standards

Conflict of interest The authors declare that they have no conflict of interest.

References

1. Commission IE (2007) Efficient electrical energy transmission and distribution. Report, Switzerland
2. Botcharova E, Heilmaier M, Freudenberger J, Drew G, Kudashow D, Martin U et al (2003) Supersaturated solid solution of niobium in copper by mechanical alloying. J Alloys Compd 351:119–125
3. Fritzemeier L (1992) High strength, high conductivity composites. Nanostruct Mater 1:257–262
4. Morris D, Morris M (1990) Mechanical alloying of copper-BCC element mixtures. Scr Metall Mater 24:1701–1706
5. Raabe D, Heringhaus F, Hangen U, Gottstein G (1995) Investigation of a Cu-20 mass% Nb in situ composite, part I: fabrication, microstructure and mechanical properties. Z Metall 86:405–415
6. Huang Q, Song Y, Sun X, Jiang L, Pong PW (2014) Magnetics in smart grid. IEEE Trans Magnet 50:1–7
7. Dupouy F, Snoeck E, Casanove M, Roucau C, Peyrade J, Askenazy S (1996) Microstructural characterization of high strength and high conductivity nanocomposite wires. Scr Mater 34:1067–1073
8. Spencer K, Lecouturier F, Thilly L, Embury JD (2004) Established and emerging materials for use as high-field magnet conductors. Adv Eng Mater 6:290–297
9. Thilly L, Veron M, Ludwig O, Lecouturier F, Peyrade J, Askénazy S (2002) High-strength materials: in-situ investigations of dislocation behaviour in Cu-Nb multifilamentary nanostructured composites. Philos Mag A 82:925–942
10. Vidal V, Thilly L, Lecouturier F, Renault P-O (2007) Cu nanowhiskers embedded in Nb nanotubes inside a multiscale Cu matrix: the way to reach extreme mechanical properties in high strength conductors. Scr Mater 57:245–248
11. Vidal V, Thilly L, Van Petegem S, Stuhr U, Lecouturier F, Renault P-O et al (2009) Plasticity of nanostructured Cu–Nb-based wires: Strengthening mechanisms revealed by in situ deformation under neutrons. Scr Mater 60:171–174
12. Lei R, Wang M, Li Z, Wei H, Yang W, Jia Y et al (2011) Structure evolution and solid solubility extension of copper–niobium powders during mechanical alloying. Mater Sci Eng A 528:4475–4481
13. Datta A, Soffa W (1976) The structure and properties of age hardened Cu-Ti alloys. Acta Metall 24:987–1001
14. Dutkiewicz J (1977) Electron microscope study of the effect of deformation on precipitation and recrystallization in copper-titanium alloys. Metall Trans A 8:751–761
15. Eze AA, Jamiru T, Sadiku ER, Durowoju MO, Kupolati WK, Ibrahim ID et al (2018) Effect of titanium addition on the microstructure, electrical conductivity and mechanical properties of copper by using SPS for the preparation of Cu-Ti alloys. J Alloys Compd 736:163–171
16. Knights R, Wilkes P (1973) The precipitation of titanium in copper and copper-nickel base alloys. Acta Metall 21:1503–1514
17. Laughlin DE, Cahn JW (1975) Spinodal decomposition in age hardening copper-titanium alloys. Acta Metall 23:329–339
18. Michels H, Cadoff I (1972) Levine E. Precipitation-hardening in Cu-3.6 wt PCT Ti. Metall Trans 3:667–674
19. Nagarjuna S (2004) Thermal conductivity of Cu-4.5 Ti alloy. Bull Mater Sci 27:69–71

20. Nagarjuna S, Balasubramanian K, Sarma DS (1995) Effects of cold work on precipitation hardening of Cu-4.5 mass% Ti alloy. Mater Trans JIM 36:1058–1066
21. Nagarjuna S, Srinivas M, Balasubramanian K, Sarmat D (1997) Effect of alloying content on high cycle fatigue behaviour of Cu-Ti alloys. Int J Fatigue 19:51–57
22. Saarivirta M (1963) High conductivity copper alloys—parts I-III. Met Ind 103:685–688
23. Saarivirta M, Cannon H (1959) Copper-titanium alloys. Met Prog 76:81–84
24. Saji S, Hornbogen E (1978) Combined recrystallization and precipitation reactions in a Cu-4 wt. percent TI-alloy. Z Metall 69:741–746
25. Suzuki S, Hirabayashi K, Shibata H, Mimura K, Isshiki M, Waseda Y (2003) Electrical and thermal conductivities in quenched and aged high-purity Cu–Ti alloys. Scr Mater 48:431–435
26. Eze A, Jamiru T, Sadiku E, Diouf S, Durowoju M, Ibrahim I et al (2017) Electrical conductivity of Cu and Cu-2vol.% Nb powders and the effect of varying sintering temperatures on their mechanical properties using spark plasma sintering. Silicon 9:855–865
27. Harbison JP, Bevk J (1977) Superconducting and mechanical properties of insitu formed multifilamentary Cu-Nb3Sn composites. J Appl Phys 48:5180–5187
28. Karasek KR, Bevk J (1979) High temperature strength of in situ formed Cu-Nb multifilamentary composites. Scr Metall 13:259–262
29. Karasek KR, Bevk J (1981) Normal-state resistivity of insitu–formed ultrafine filamentary Cu-Nb composites. J Appl Phys 52:1370–1375
30. Verhoeven J, Downing H, Chumbley LS, Gibson E (1989) The resistivity and microstructure of heavily drawn Cu-Nb alloys. J Appl Phys 65:1293–1301
31. Verhoeven J, Finnemore D, Gibson E, Ostenson J, Goodrich L (1978) Superconducting properties of insitu prepared Nb-Cu-Sn alloys. Appl PhysLett 33:101–102
32. Eze AA, Jamiru T, Sadiku ER, Durowoju MO, Kupolati WK, Ibrahim ID et al (2017) Effect of titanium addition on the microstructure, electrical conductivity, thermal conductivity and mechanical properties of copper by using SPS for the preparation of Cu-Ti alloys. J Alloys Compd
33. Dadras M, Morris D (1997) Examination of some high-strength, high-conductivity copper alloys for high-temperature applications. Scr Mater 38:199–205
34. Lei R, Xu S, Wang M, Wang H (2013) Microstructure and properties of nanocrystalline copper–niobium alloy with high strength and high conductivity. Mater Sci Eng A 586:367–373
35. Jinyong Z, Tianya T, Zhengyi F, Weimin W (2005) The densification of Cu/Ti system by spark plasma sintering. J Wuhan Univ Technol Mater Sci Ed 20:83–85
36. Wang L, Pouchly V, Maca K, Shen Z, Xiong Y (2015) Intensive particle rearrangement in the early stage of spark plasma sintering process. J Asian Ceram Soc 3:183–187
37. Li Y, Han W, Chen G, Cheng Y, Gui K (2016) Effect of Cu particles on phase transformation of spark plasma sintered silicon nitride. Mater Lett 174:122–125
38. Liu C, Chen J-S (2002) Low leakage current Cu (Ti)/SiO_2 interconnection scheme with a self-formed TiO x diffusion barrier. Appl Phys Let. 80:2678–2680
39. Jiménez YS, Gil MT, Guerra MT, Baltes L, Rosca JM (2009) Interpretation of open circuit potential of two titanium alloys for a long time immersion in physiological fluid. Bull Transilvania Univ Braşov 2:51